The evolution of the Alberta Complex, Naub Diorite and Elim Formation within the Rehoboth basement inlier, Namibia: geochemical constraints

Thomas Becker[1] and Arnd Brandenburg[2]

[1]*Geological Survey of Namibia, P.O. 2168, Windhoek, Namibia; e-mail: tom@mme.gov.na*

[2]*DESY Theory Group, D-22603 Hamburg, Germany; e-mail: Arnd.Brandenburg@desy.de*

Evolution of the Palaeoproterozoic Rehoboth Sequence within the Rehoboth Basement Inlier of Namibia probably documents transition from arc to back arc regions within an Eburnian magmatic arc. New field evidence suggests a stratigraphic position of the arc-related Gaub Valley Formation in the lower portion of the Rehoboth Sequence. This is overlain by the shallow marine back-arc related Elim Formation. Sedimentation was accompanied by mafic hyaloclastic volcanism. Geochemical analyses of these volcanics reveal their subalkaline, tholeiitic nature as well as local strong alteration by hydrothermal or metamorphic overprinting. REE-patterns remain unaffected and exhibit depletion of HREE, relatively to MORB, while LREE are slightly enriched. Pronounced negative spikes of Zr and Hf, minor to no depletion of Nb, Ti and Ta as well as normal enrichment of LILE are in accordance with modern back arc basalts in areas with minor subduction influence. The Gaub Valley Formation and basal Elim Formation were intruded by calc-alkaline, subduction-related dioritic to tonalitic magmas, the Naub and Weener plutons. Close spatial and temporal linkage must be assumed between the Elim and Gaub Valley Formations, as well as a rapid change from subduction zone to back arc magmatism. Alternatively, different source regions may have been active at the same time. Subsequently, the Elim Formation was intruded by the ultramafic to mafic layered Alberta Complex. Cumulate layers of plagioclase, olivine and pyroxene predominate within the interior of this body. However, gabbroic rocks from the Marginal Zone display affinity to mafic volcanics of the Elim Formation, which may be due either to AFC processes or to an origin from the same source. Modelling, based on fractional crystallisation, shows that rocks of the Alberta Complex can be genetically linked to the volcanic rocks of the Elim Formation by extracting varying amounts of ol, opx, cpx and plag and mixing them with minor amounts of fractionated liquid.

Introduction

The Rehoboth Basement Inlier (RBI) in central Namibia comprises magmatic and sedimentary rocks of various ages and origins. Geochronological data indicate three major crust-forming events, which correspond at a regional scale to the Palaeoproterozoic Eburnean-Ubendian (~2.2 -1.8 Ga), the Mesoproterozoic Kibaran (~1.3-1.1 Ga) and the Neoproterozoic Pan-African (~0.7 to 0.5 Ga) cycles. Within the RBI, the Eburnian-Ubendian cycle is represented by volcano-sedimentary formations and high-grade metamorphic complexes of assumed pre-Rehoboth Sequence age (Neuhof, Elim Formations, Mooirivier Complex) and the *ca.* 1800 Ma Rehoboth Sequence (Marienhof, Billstein and Gaub Valley Formations). Deposition of these units was accompanied, or followed, by major plutonism ranging in composition from ultramafic to mafic (Alberta, Doornboom Complexes) through intermediate (Weener Suite, Naub diorite) to granitic (Piksteel Suite; Table 1). Figure 1 shows the extent and distribution of these Palaeoproterozoic units.

Recent fieldwork and new geochronological data have led to a revision of the existing stratigraphy. Pre-Rehoboth and Rehoboth units are now thought to relate to only one tectono-magmatic event, and their relative stratigraphic positions are re-arranged (Table 1). The Rehoboth Sequence is interpreted as being concomitant with an Eburnian-Ubendian magmatic arc (Master, 1993; Becker *et al.*, 1996) and the sedimentary history probably reflects transition from arc to back arc environment: (1) Terrestrial clastic sediments and bimodal volcanics of the Neuhof Formation are considered to immediately pre-date the Rehoboth Sequence and may document initial rifting behind the arc. Unfortunately, no geochronological or geochemical information currently exists on these volcanics whose stratigraphic position remains doubtful. (2) Advanced rifting, still within a terrestrial environment, is assumed for the deposition of the Gaub Valley Formation (GVF). This unit comprises a thick stack of fluviatile-lacustrine sediments at the base, overlain by volcanic-derived sediments and metatuffites varying in composition from andesitic to rhyolitic. Geochemical analysis of these volcanics and of the coeval Weener Suite clearly suggest a subduction environment (Becker, 1995). (3) The GVF is overlain with a transitional and partly tectonised contact by the Elim Formation which formed in a shallow marine depositional environment. At the base, the Elim Formation comprises quartz-sericite schist, quartzite and meta-arkose. Higher up in the stratigraphy it grades into metamorphic greywacke, arkose, carbonate, calc-silicate rocks, magnetite quartzite (itabirite) and minor mafic volcanic rocks. Major mafic volcanism prevailed at the top of the Elim Formation (Brewitz, 1974) and was accompanied by subordinate silicic pyroclastic eruptions. (4) Finally, the youngest unit of the Rehoboth Sequence, the Marienhof Formation, consists of clastic sediments which marks the final stage of basin fill. The Mooirivier Metamorphic Complex is considered to represent highly metamorphosed equivalents of the Elim Formation and is referred to as the Mooirivier Member in this paper (Table 1).

This paper describes petrologic and geochemical features of various intermediate to mafic igneous rocks of the Rehoboth Sequence in order to (1) define more precisely the Palaeoproterozoic geodynamic history of the RBI, (2) determine the different sources involved in the evolution of the magmas involved, and (3) establish possible links between the various igneous suites within

Table 1: Presentation of present stratigraphy from SACS (1980) and modified stratigraphy which is based on new field evidence and geochronological data

Present stratigraphy (SACS, 1980)		**Modified stratigraphy**		**Intrusives**	**Age [Ma]**	**Method**	**Ref**
Sinclair Sequence		Sinclair Sequence		Gamsberg Granite Suite	1099 ± 24	U/Pb zircon	3
	Nuckopf Fm		Nuckopf Fm Billstein Fm		1221+/-33	U/Pb zircon	7
Rehoboth Sequence		Rehoboth Sequence		Piksteel Granite	1645 ± 41	U/Pb zircon	7
	Gaub Valley Fm						
	Billstein Fm						
	Marienhof Fm		Marienhof Fm				
				Alberta Complex Naub Diorite Weener Tonalite	1759±144 1725 ± 25 1765 ± 21	Sm/Nd wr Rb/Sr wr U/Pb zircon	8 2 5
pre-Rehoboth units	Elim Fm		Elim Fm including Kamasis Member & Moorivier Member		1820+/- 184 1764 ± 56 1725 ± 10	Sm/Nd wr U/Pb sphene U/Pb zircon	4 8 5
	Neuhof Fm		Gaub Valley Fm		1782 ± 10	U/Pb zircon	6
	Mooirivier Complex		Neuhof Fm		1784 ± 45	U/Pb zircon	1

References: **1**: Burger and Walraven (1978); **2**: Reid *et al*. (1988); **3**: Pfurr *et al*. (1991); **4**: Ziegler and Stoessel, 1993; **5**: Becker *et al*. (1996); **6**: Nagel *et al*. (1996); **7**: Hilken (1998); **8**: Becker *et al*. (subm.)

the RBI. The evolution of the Rehoboth Sequence outlined above should be reflected in the geochemistry of the igneous rocks. It was anticipated that, if the model applies, a trend should be seen from subduction influenced patterns of the initial back arc towards MORB composition within progressive opening of the back arc (Fryer *et al.*, 1990).

Petrography and Geochronology

Mafic igneous rocks of the Elim Formation

Mafic igneous rocks of the Elim Formation are exposed throughout the RBI. Major outcrops occur on the farms Samkubis 516 and Kobos 321 about 30 km west of Rehoboth where thicknesses reach several hundred

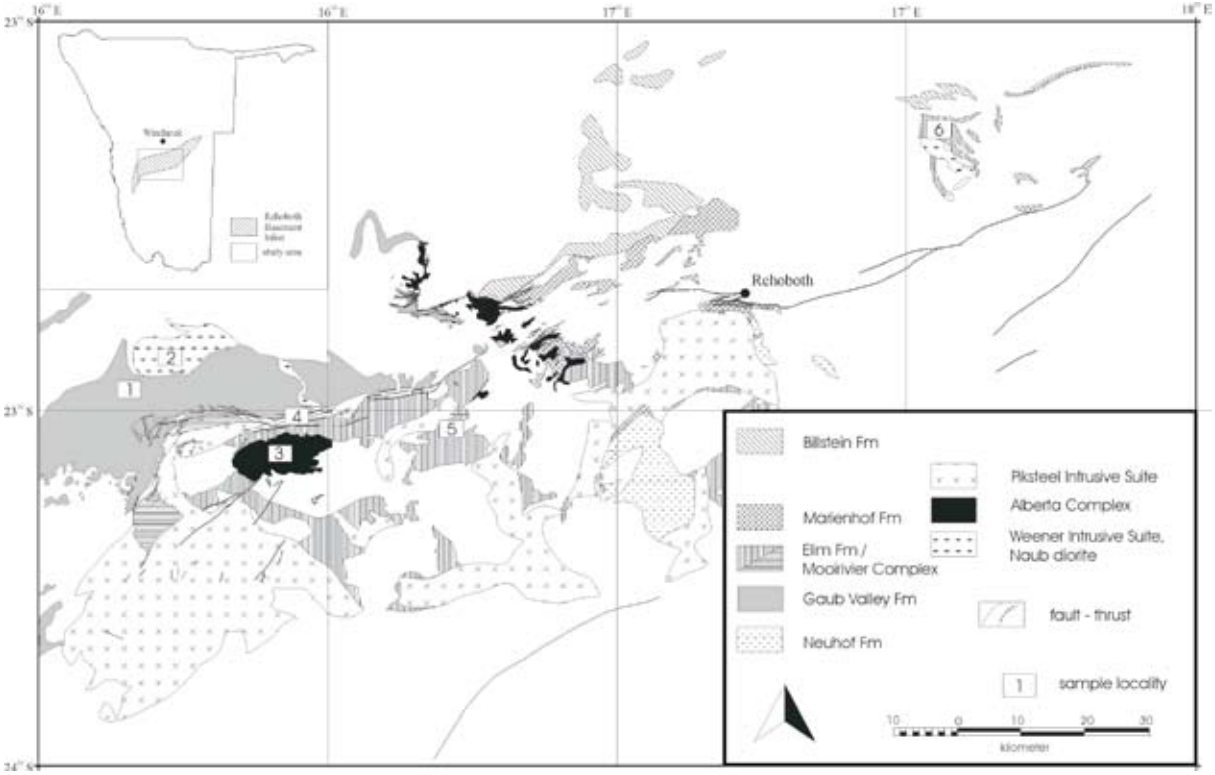

Figure 1: Geological map of the Rehoboth area - paleoproterozoic units and sample localities. (1) Gaub Valley Formation (2) Weener Igneous Complex (3) Alberta Complex (4) Elim Formation - Areb (5) Elim Formation - Kobos (6) Elim Formation - Samkubis (7) Elim Formation and Naub Diorite

metres (Fig. 1). In places, amygdaloidal layers, pyroclastic lenses and crumpled scoriaceous surfaces can be recognised. Apart from originally fine-grained rocks, layers of coarse-grained structureless amphibolite are found locally which may represent altered basic sills. On Kobos 321, fragmented hyaloclastic mafic volcanics are interbedded with quartz-mica schists which host a volcanogenic massive Cu-Zn sulphide deposit, the former Kobos mine (Brewitz, 1974). Vesicle-rich, felsic, angular pumice fragments within a dark, fine-grained matrix indicate shallow water conditions during deposition.

Two stages of metamorphism have been described within the Elim Formation. An early prograde metamorphism reached amphibolite grade, while the present mineral assemblage is the result of retrograde metamorphism, with amphiboles being replaced by tremolite, actinolite, talc and chlorite. Minor components comprise epidote, clinozoisite, calcite and quartz, which partly have replaced plagioclase. Magnetite and pyrite are locally abundant while ilmenite and sphene are accessory components. The recrystallised lava displays a wide variety of textures comprising hornblende fels, fine-grained amphibole schist and granular mottled amphibolite. In many of these lithotypes, a fine mineral banding is caused by variations in hornblende content.

The few geochemical data available of the mafic volcanics show affinity to subalkaline tholeiitic basalts (Ziegler and Stoessel, 1993). Due to limited data, no specific tectonic environment could be assigned to their evolution. Whole-rock Sm/Nd analysis yielded T_{DM} ages of 1686 to 2373 Ma while T_{CHUR} ages vary between 643 and 1382 Ma. A reference line calculated through five data points resulted in an age of 1820 ± 184 Ma (ε_{Nd} = 3.8 ± 3.4). One U-Pb sphene age of 1764 ± 56 Ma was obtained from rare calcsilicates on the farm Grauwater 341, which are thought to be metamorphosed lava (Becker *et al.*, subm.).

Alberta Complex

All units of the Rehoboth Sequence are intruded by a series of mafic to ultramafic and, in places, layered intrusions of which the Alberta Complex is the most prominent. It is situated *ca.* 140 km southwest of Windhoek, immediately to the south of the Areb Shear Zone, a prominent shear belt that defines the boundary between the Southern Margin Zone and the Southern Foreland of the Pan-African Damara Orogen (Fig. 1). The intensely faulted complex forms an oval-shaped body some 16 km in length and 6.5 km in width. It is essentially composed of a thick succession of layered gabbroic rocks (Layered Sequence), which were intruded at a later stage by a pegmatoid phase, as well as by harzburgite and dunite (de Waal, 1966). The Layered Sequence has been subdivided into four zones, e.g. Marginal Zone, Basal Zone, Central Zone, and Upper Zone. They are thought to represent individual magmatic pulses. The boundaries between individual zones are marked by screens of country rock and/or sudden appearence of fine banding. Finely banded layering, in general, is confined to the base of each zone and later grades into medium- to coarse-grained amphibolites and metagabbros without any primary magmatic textures.

Paleoproterozoic rocks of this area have been subjected to at least three stages of metamorphism: (1) An early assemblage of diopside, wollastonite and garnet (andradite) forming crystal aggregates up to 5 cm across occurs in Ca-rich country rock of the Elim Formation and Mooirivier Complex. This first alteration was probably due to contact rather than regional metamorphism being supported by the absence of high-grade minerals (e.g. cordierite, sillimanite, andalusite). Possible thermal sources are the Alberta Complex or the nearby granitoid Piksteel Suite (Fig. 1); (2) A first regional metamorphic event is indicated by the mineral assemblage hornblende and plagioclase and a penetrative gneissic fabric imparted on all rocks of paleoproterozoic age;

Table 2: Results of the XRF analyses (nd = not determined). Analysis of samples EFAR01-06 by Boehm (1998)

Sample	MZ01	MZ02	EFKO01	EFKO02	EFKO03	EFKO04	EFKO05	EFKO06	EFAR01	EFAR03	EFAR04	EFAR05	EFAR06	ND01
Farm	Alberta	Alberta	Kobos	Kobos	Kobos	Kobos	Kobos	Kobos	Areb	Areb	Areb	Areb	Areb	Naub
Lithology	gabbro	gabbro	amphibolite	chl-schist	chl-schist	chl-schist	chl-schist	chl-schist	amphibolite	amphibolite	amphibolite	amphibolite	amphibolite	diorite
SiO2	49.8	45.9	56.3	47.1	44.6	46.2	48.1	45.3	48.2	50.3	47.8	48.3	50.2	59.2
TiO2	0.81	0.29	0.68	1.02	1.08	0.90	1.05	0.90	1.35	0.95	1.34	1.08	0.77	0.64
Al2O3	18.2	22.7	14.8	10.3	10.5	9.33	10.5	9.23	15.4	13.4	15.6	16.6	14.2	16.2
Fe2O3	11.3	7.16	9.69	11.5	10.5	11.4	12.9	12.1	11.7	14.1	11.5	10.6	12.4	7.82
MnO	0.15	0.12	0.15	0.19	0.17	0.23	0.25	0.15	0.17	0.20	0.17	0.19	0.19	0.14
MgO	5.45	5.04	4.72	4.58	4.39	4.87	6.95	6.43	7.39	6.47	7.35	6.73	6.84	2.64
CaO	10.14	13.35	7.18	19.3	20.0	20.9	15.3	19.7	10.9	10.4	11.2	11.8	10.4	5.9
Na2O	2.85	2.00	3.66	1.73	1.79	1.07	1.24	1.05	2.00	1.72	2.01	1.90	1.10	3.25
K2O	0.2	0.41	0.17	0.48	0.43	0.07	0.26	0.6	0.05	0.43	0.1	0.11	0.51	2.41
P2O5	0.06	0.04	0.20	0.17	0.15	0.15	0.17	0.14	0.12	0.09	0.20	0.09	0.07	0.30
SO3	<0.01	<0.01	<0.01	<0.01	<0.01	0.03	<0.01	<0.01	nd	nd	nd	nd	nd	<0.01
Cl	0.048	0.009	<0.001	0.002	0.005	0.003	0.003	0.002	nd	nd	nd	nd	nd	0.007
F	0.104	<0.02	<0.02	0.074	<0.02	<0.02	<0.02	<0.02	nd	nd	nd	nd	nd	0.149
LOI	0.81	2.73	2.28	3.24	6.04	4.55	2.94	3.97	nd	nd	nd	nd	nd	1.01
Sum	99.82	99.78	99.81	99.65	99.64	99.65	99.65	99.60	97.30	98.03	97.22	97.43	96.68	99.68

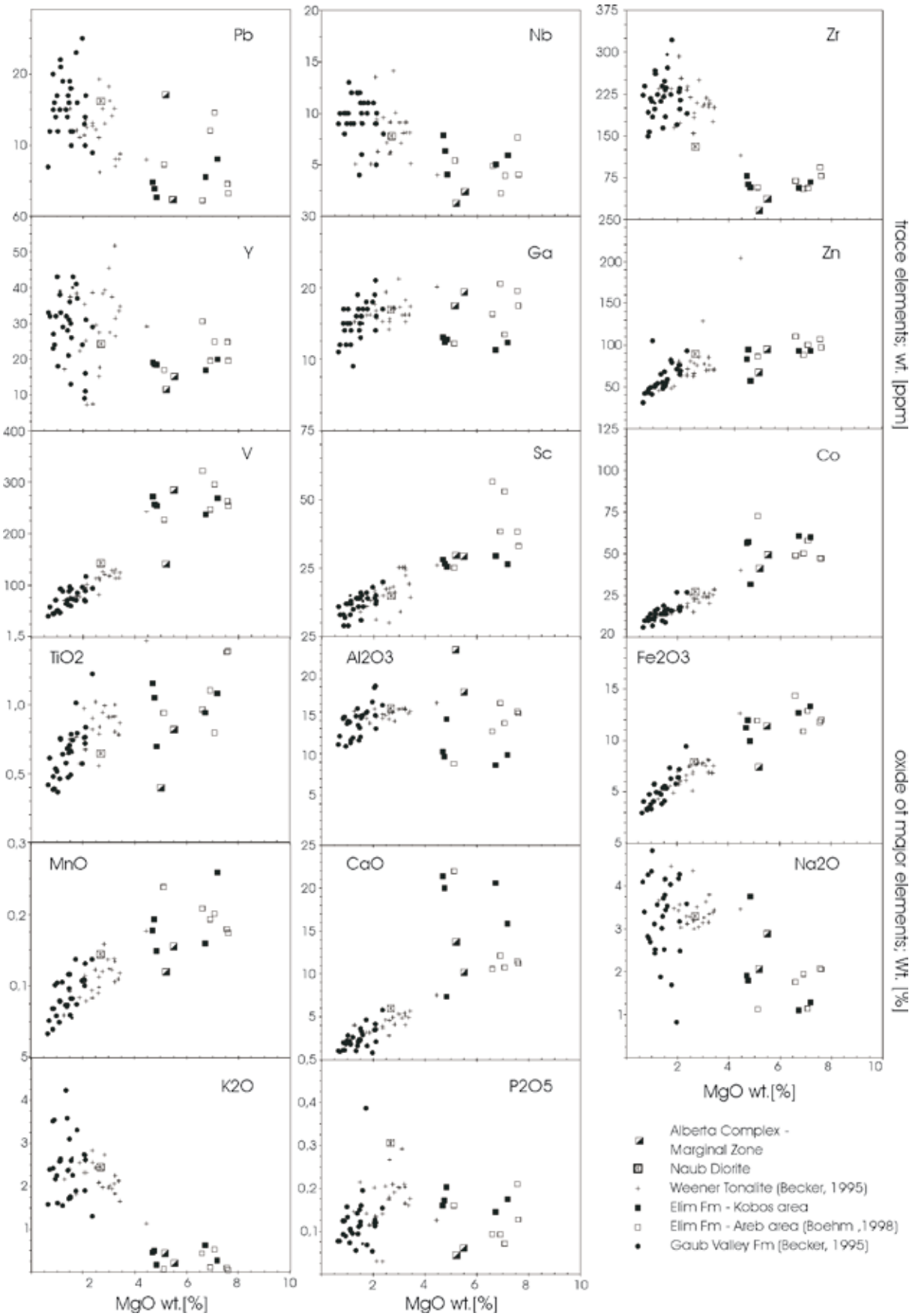

Figure 2: Presentation of geochemical data in MgO Harker diagrams. Compatibility of TE decreases from left to right and from top to bottom.

(3) Greenschist facies retrograde metamorphism during Damara time formed a mineral paragenesis of epidote, chlorite and tremolite. In areas of high shear (i.e. Nauams fault, Fig. 2), serpentinite is altered to talc or asbestiform tremolite, while feldspar has decomposed to sericite.

One Rb/Sr whole rock age of 1442 ± 32 Ma (Reid *et al.*, 1988) is rather ambiguous, because of the possibility of overprinting during Pan-African metamorphism. Even Sm/Nd isotope systematics are difficult to interpret. A reference line calculated through seven data points resulted in an age of 1759 ± 144 Ma with ε = 1.3 ± 3.6 (Becker *et al.*, subm.). Geochemical data are limited to a few major element analyses, together with Cr and Ni (de Waal, 1966). Therefore, no specific geotectonic setting has so far been assigned for this intrusion.

Naub Diorite

The Naub Diorite is a prominent unit of a magmatic suite which ranges in composition from gabbro through diorite to granodiorite and occurs throughout the Palaeoproterozoic domains of the RBI. The type area is situated east of Rehoboth in the vicinity of the Dubis Mountains, where the magma intruded metasediments and basic metalavas of the Elim Formation as well as granite- injected schist and quartzite of supposed pre-Elim age (Schalk, 1988). After first being subjected to regional amphibolite facies metamorphism, the Naub Diorite was in turn intruded by granites of Mesoproterozoic age. Generally strongly sheared and gneissic in appearance, the texture of the diorite remains hypidiomorphic-granular in less deformed domains, varying from fine to medium grained. Major components comprise plagioclase (oligoclase to andesine) and two types of hornblende, while quartz, biotite, magnetite, ilmenite and apatite occur in minor to accessory amounts. More mafic amphibolites and pegmatitic amphibole fels occur as irregular sheets several hundred metres long and up to 50 m wide north of Dubis Mountain. They are composed predominantly of hornblende with subordinate plagioclase. The amphibole fels comprises a fine-grained groundmass of intergrown hypidiomorphic plagioclase and subhedral hornblende, with abundant euhedral hornblende crystals up to 5 cm long. These felses may represent an early cumulate phase of the Naub intrusion because they are intruded by more evolved diorite of the main body. One Rb/Sr whole-rock sample yielded an age of 1725 ± 25 Ma and $^{87}Sr/^{86}Sr$-initial of 0.7041 ± 3 (Reid *et al.*, 1988). Petrographic and isotopic compositions show similarity with the Weener Igneous Complex (WIC) about 100 km to the west (Fig. 1). The latter intrusion has yielded a conventional U-Pb zircon age of ~1768 ± 11 Ma, and is related to subduction zone magmatism (Becker *et al.*, 1996, Becker *et al.*, 2000).

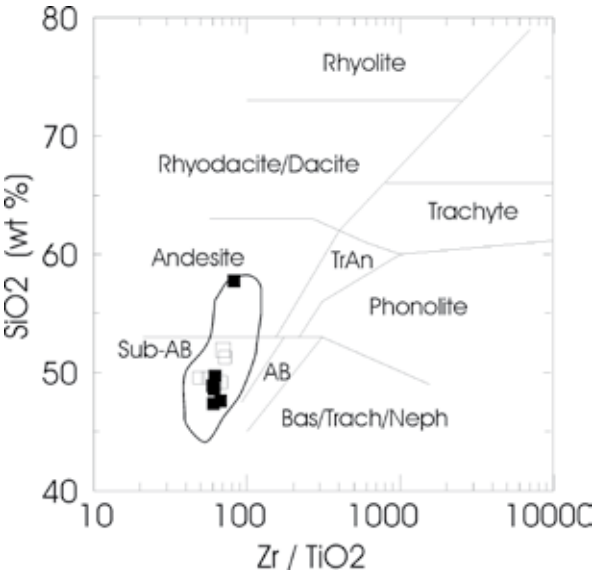

Figure 3: Presentation of sample from the Elim Formation in the SiO_2 vs Zr/TiO_2 classification diagram after Winchester and Floyd, 1977 (for legend see Fig. 3). Analyses scatter from subalkaline basalts to andesites

Geochemistry

Methods

Analytical work was carried out by the Federal Institute for Geoscience and Natural Resources (BGR) Hannover, and the Institute for Geochemistry, University of Goettingen (Germany). Sample weights were between five and 25 kg. Major and trace elements were determined by XRF. REE and HFSE were analysed by ICP-MS. Analytical procedures were described by Heinrichs and Herrmann (1990). Analytical errors for ICP-MS are <5% [rel.] (BGR) and 20% [rel.] (Goettingen). Analytical errors for XRF are generally <1% [rel.] for major elements and <5% [rel.] for trace elements.

XRF analyses are listed in Table 2, while trace elements determined by ICP-MS are listed in Table 3. Sample locations are given in Figures 1 and 2. Sampling of the Elim Formation took place in two areas, viz. the basal part of the Elim Formation on the farm Areb 176 close to the Alberta Complex (Boehm, 1998) and higher up in the stratigraphy on the farm Kobos 321 (Figs. 1 and 2). The Alberta Complex has been sampled along several profiles which cover all units of the Layered Sequence (Fig. 2). Additional samples have been taken from the cone sheet and from pyroxenitic rocks which occur as pIUGS and sills. One sample from the Naub Diorite mainly served to allow comparison with the Weener and Alberta Complexes.

Elim Formation

Classification

Mafic rocks from the basal (Areb 176) and upper (Kobos 321) Elim Formation differ significantly in composition (Fig. 2, Tables 2, 3). While both groups display narrow ranges in SiO_2 [47 -53 %], Fe_2O_3 [10.9 -

14.4 %] and MgO [4.7-7.6 %], samples from the Kobos area contain increased concentrations of CaO [16-21 %] vs. [11.75-12.1% - Areb], Ba [200-450ppm] vs. [20-120ppm - Areb], Ni [166-236 ppm] vs. [40–142 ppm - Areb], Cr [590-805 ppm] vs [115-355 ppm] and considerably less Al_2O_3 [9.6-10.9%] vs. [13.7-17.1% - Areb]. Extremely high CaO combined with increased Ni and Cr and comparatively low Al, Mg and Cu clearly indicate strong alteration of the hyaloclastic rocks of the Kobos area. In addition, major alteration of the original rock composition is indicated by Harker diagrams which show random scatter, even for elements which are normally well correlated. Therefore, magmatic lines of descent are totally disturbed. However, analyses of Ziegler and Stoessel (1993) from the Kobos area are similar to those from Areb 176 and show that subalkaline, tholeiitic magmatism prevailed throughout deposition of the Elim Formation. This is documented by high Y/Nb [2.5, 9] and high Zr/P_2O_5 [280, 780] ratios, as well as relatively low TiO_2 [0.7, 1.4] and P_2O_5 [0.07, 0.2] (Fig. 3).

Figure 4 shows the N-MORB-normalised spidergram of trace elements. The most noticeable features of the diagram are: (1) Element patterns from the Kobos and Areb areas overlap and are aligned nearly parallel to each other suggesting that they could be related through low-pressure fractional crystallisation; (2) Generally smooth enrichment occurs from the mildly incompat-

Table 3: Results of ICP-MS analyses (nd = not determined). Analysis of samples EFAR01-06 by Boehm (1998)

Sample	MZ01	MZ02	EFKO01	EFKO02	EFKO03	EFKO04	EFKO05	EFKO06	EFAR01	EFAR03	EFAR04	EFAR05	EFAR06	ND01
Farm	Alberta	Alberta	Kobos	Kobos	Kobos	Kobos	Kobos	Kobos	Areb	Areb	Areb	Areb	Areb	Naub
Lithology	gabbro	gabbro	amphibolite	chl-schist	chl-schist	chl-schist	chl-schist	chl-schist	amphibolite	amphibolite	amphibolite	amphibolite	amphibolite	Diorite
Ag	0.03	0.05	0.02	0.10	0.10	0.30	0.08	0.07	nd	nd	nd	nd	nd	0.084
As	0.81	0.67	1.64	2.76	5.90	9.54	2.78	4.60	nd	nd	nd	nd	nd	1.62
Ba	66.4	104	79.2	415.0	382	42.0	192	307	14.8	81.4	128	14.6	57.7	728
Be	0.330	0.230	0.440	0.340	0.350	0.320	0.380	0.320	0.366	0.430	0.538	0.662	0.478	1.26
Bi	0.035	0.069	0.036	0.030	0.035	0.180	0.086	0.068	0.001	0.026	0.002	0.102	0.021	0.16
Cd	0.091	0.180	0.042	0.130	0.110	0.160	0.160	0.130	nd	nd	nd	nd	nd	0.078
Ce	12.60	10.00	14.90	17.90	17.60	14.30	15.80	13.70	17.31	14.25	26.75	10.91	12.28	55.2
Co	37.8	27.1	22.9	39.3	37.7	43.6	40.2	46.2	nd	nd	nd	nd	nd	15.9
Cr	33	140	62	468	541	586	491	1290	nd	nd	nd	nd	nd	21
Cs	0.034	0.170	0.045	0.025	0.055	0.027	0.053	0.066	2.194	1.019	0.655	0.799	2.544	1.42
Cu	46.7	37.9	19.3	83.9	91.9	200	89.4	80.1	nd	nd	nd	nd	nd	61.2
Ga	19.0	16.9	12.4	11.9	12.2	11.6	11.9	10.8	nd	nd	nd	nd	nd	16.7
Hf	0.56	0.45	1.45	1.34	1.45	0.85	1.04	0.78	0.75	0.86	1.01	0.61	0.65	2.10
In	0.062	0.04	0.047	0.056	0.057	0.057	0.059	0.054	nd	nd	nd	nd	nd	0.051
La	5.24	3.71	6.18	7.53	7.27	6.01	6.66	5.57	6.29	6.54	10.6	3.69	4.86	27.9
Li	6.07	7.88	8.61	2.34	2.13	1.89	1.20	3.56	18.0	13.4	14.9	21.9	20.1	11.1
Mn	1670	687	769	756	729	1800	1760	683	nd	nd	nd	nd	nd	657
Mo	0.39	0.53	0.59	0.54	0.72	0.75	0.48	0.49	0.13	0.25	0.44	0.36	0.27	0.69
Nb	2.35	1.31	3.96	6.12	7.37	5.14	5.72	4.82	3.94	4.79	7.42	2.16	3.83	7.68
Ni	22.7	31.5	22.1	130	131	191	160	208	nd	nd	nd	nd	nd	10.3
Pb	2.44	16.6	2.69	3.81	4.59	6.98	7.86	5.37	3.20	2.27	4.50	11.77	14.12	16.0
Rb	3.17	16.6	2.39	4.84	6.51	0.49	1.71	5.46	nd	nd	nd	nd	nd	58.3
Sb	0.04	0.11	0.32	0.33	0.50	0.87	0.62	0.46	nd	nd	nd	nd	nd	0.19
Sc	29.0	28.9	24.9	25.6	26.3	23.9	25.6	28.2	32.1	55.3	37.2	37.4	51.2	14.7
Se	0.30	0.00	0.74	0.26	0.11	0.18	0.12	0.00	nd	nd	nd	nd	nd	0.23
Sn	1.83	17.8	0.98	1.28	1.33	1.71	1.45	2.23	0.70	0.76	0.68	0.63	0.62	2.08
Sr	171	176	240	211	208	188	236	243	nd	nd	nd	nd	nd	629
Ta	0.19	0.12	0.27	0.40	0.48	0.34	0.38	0.31	1.08	0.76	1.06	0.143	1.35	0.44
Th	0.32	0.08	0.91	0.73	0.79	0.61	0.62	0.56	0.32	0.74	0.46	0.05	0.66	7.04
Ti	3890	1310	2670	3180	3360	2680	3380	2830	nd	nd	nd	nd	nd	2370
Tl	0.014	0.027	0	0	0.01	0	0	0	0.016	0.022	0.013	0.025	0.051	0.16
U	0.090	0.026	0.29	0.22	0.25	0.20	0.21	0.18	0.16	0.20	0.15	0.07	0.65	0.88
V	271	131	221	203	202	177	210	224	nd	nd	nd	nd	nd	133
W	0.12	0.19	0.20	0.69	0.59	0.61	0.39	0.52	2.20	1.79	1.62	1.87	1.33	0.38
Y	15.00	11.1	18.0	17.9	17.8	16.1	19.3	16.1	16.8	24.9	21.9	14.5	22.1	23.9
Zn	87.3	63.7	53.8	77.2	77.2	70.2	85.7	81.5	nd	nd	nd	nd	nd	81.9
Zr	14.70	8.43	55.9	48.1	53.2	27.4	34.1	22.4	76	68	91	53	54	75.4
Pr	1.67	1.34	1.96	2.41	2.42	1.99	2.21	1.91	2.42	1.98	3.45	1.57	1.53	7.36
Nd	7.42	5.68	8.74	10.7	10.9	9.15	10.3	8.77	11.0	8.38	14.4	7.23	6.65	29.0
Sm	2.00	1.39	2.26	2.76	2.83	2.45	2.78	2.37	2.93	2.50	3.46	2.16	2.00	5.77
Eu	0.76	0.46	0.70	0.92	0.93	0.83	0.94	0.76	1.14	0.95	1.24	0.94	0.77	1.43
Gd	2.36	1.57	2.74	3.26	3.29	2.89	3.29	2.78	3.23	3.15	4.15	2.40	2.51	5.38
Tb	0.39	0.38	0.45	0.52	0.53	0.47	0.54	0.45	0.47	0.53	0.56	0.37	0.45	0.75
Dy	2.58	1.81	2.96	3.19	3.18	2.88	3.40	2.79	2.83	3.70	3.35	2.30	3.23	4.17
Ho	0.55	0.40	0.64	0.66	0.66	0.61	0.72	0.59	0.57	0.80	0.69	0.47	0.70	0.84
Er	1.62	1.19	1.95	1.84	1.87	1.69	2.06	1.68	1.52	2.32	1.91	1.29	2.03	2.44
Tm	0.24	0.18	0.30	0.27	0.27	0.24	0.30	0.24	0.22	0.37	0.28	0.19	0.33	0.37
Yb	1.63	1.20	1.98	1.71	1.72	1.56	1.93	1.53	1.44	2.55	1.87	1.30	2.18	2.33
Lu	0.26	0.20	0.33	0.28	0.28	0.24	0.31	0.25	0.20	0.39	0.27	0.19	0.34	0.39

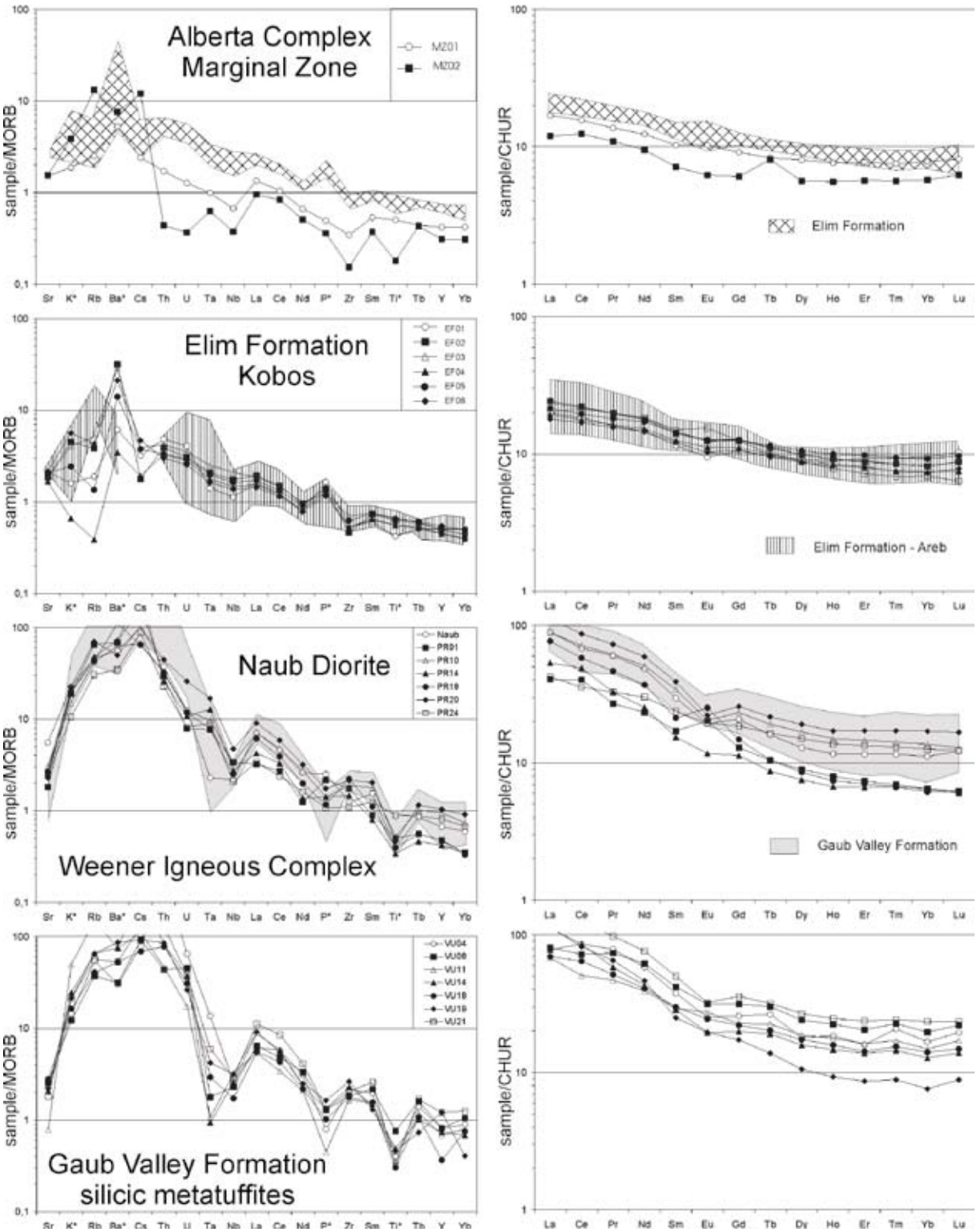

Figure 4: MORB-normalised (Hofmann, 1988) multi-element plot for silicic volcanic rocks of the Gaub Valley Formation, intermediate intrusive rocks of the Weener Igneous Complex and Naub Diorite, mafic volcanic rocks of the Elim Formation, and gabbroic rocks of the Marginal Zone (AC). CHUR-normalised REE plots are shown to the right of each diagram. For comparison the shaded areas show spread in composition of other units. (* = XRF-method, all other ICP-MS)

ible to the highly incompatible elements (right to left). Whereas mildly incompatible elements (Nd, Zr, Sm, Ti, Y, Yb) are depleted relative to N-MORB, LREE and LILE are enriched which matches patterns of E-MORB; (3) P and Ba have positive spikes and only minor negative spikes are displayed for HFSE (Ti, Zr, Nb, and Ta).

REE patterns from the Kobos area are marked by mild enrichment in LREE relative to HREE, with $[La/Lu]_N$ ratios varying from 1.93 to 2.78 and small but

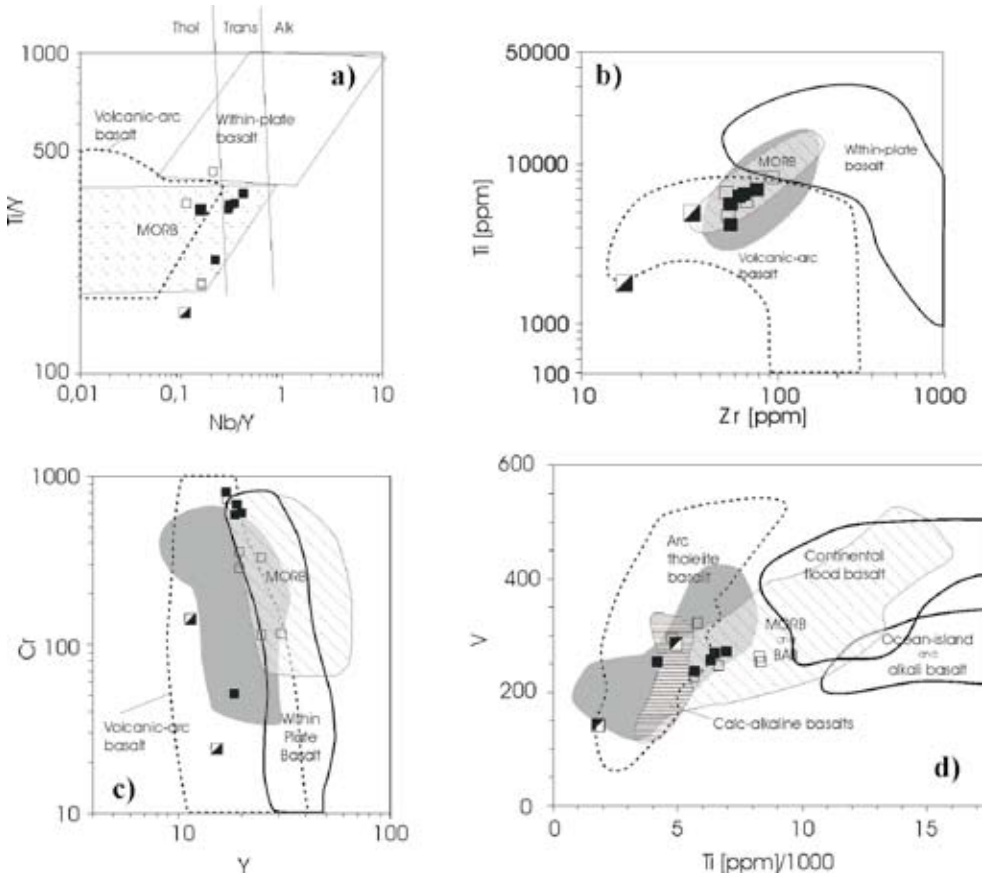

Figure 5: Presentation of samples from the Elim Formation and the Alberta Complex in discrimination diagrams for modern basalts (for legend see Fig. 2, shaded areas show data range of Ziegler and Stoessel, 1993). a: Ti/Y vs. Nb/Y (Pearce, 1982) b: Ti vs. Zr (Pearce & Cann, 1973) c: Cr vs. Y (Pearce, 1982) d: V vs. Ti/1000 (Shervais, 1982). Note consistent spread of analyses from Elim Formation within volcanic arc to MORB fields.

consistent Eu anomalies [Eu/Eu* = 0.85 - 0.95]. Hence, mantle melting was not associated with residual garnet. Samples from Areb display more variable $[La/Lu]_N$ ratios [1.5 - 4.1] and no or small positive Eu anomalies [1-1.25] which probably are the result of analytical error. Almost parallel alignment of HREE to the x-axis, and stronger enrichment of LREE approximates patterns of the Naub Diorite and Weener Igneous Complex (see below).

Comparison with modern volcanic suites

The majority of the samples from the Elim Formation plot in fields of arc-related basalts (Figs. 5a to d). However, most of these diagrams are not suitable for distinction between different regions within a volcanic arc. An exception is the Ti-V discrimination diagram of Shervais (1982). Variation in V, relatively to Ti, is a function of oxygen activity of magma and of crystal fractionation processes. These parameters, in turn, can be linked to the environment of eruption (Rollinson, 1993). Ti/V ratios between 15 and 33 suggest affinity of the Elim Formation mafic volcanics to back arc basalts or MORB. This is supported by the La/10-Y/15-Nb/8 discrimination diagram of Cabanis and Lecolle (1989) in which Elim samples plot in the fields of back arc and 'continental' basalts. In contrast, low Ce/Pb [0.8-5.5],

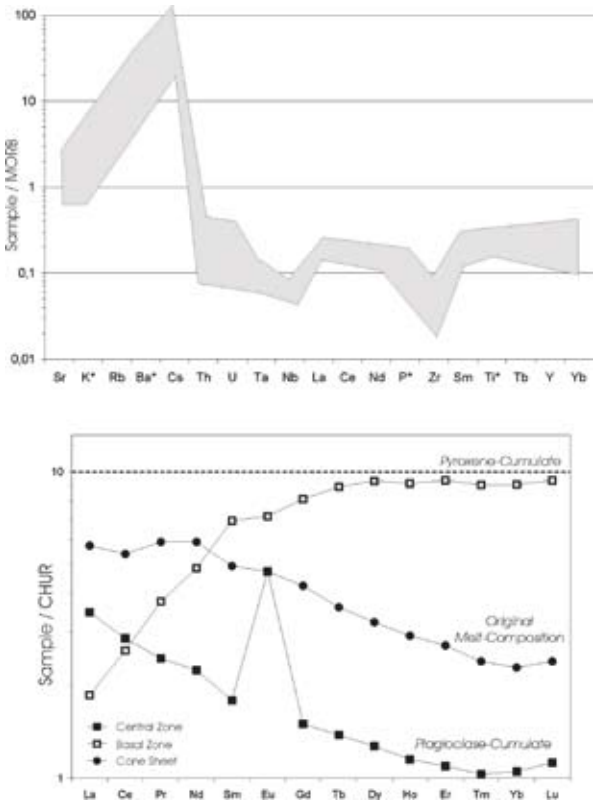

Figure 6: Principal REE patterns and shape of spidergrams for samples of the Alberta Complex

La/Yb_N [1.5-2] and K/Rb (6-127) ratios are rather characteristic for intra-oceanic arc magmatism (Gribble *et al.*, 1998).

Back arc basalt from the New Hebrides has been documented by Maillet *et al.* (1995). Variation from MORB through back arc basalts to island arc tholeiite and calc-alkaline basalt composition results from complex interaction of subduction zone magmatism and back arc spreading. Any subduction component is absent in this modern back arc area and the patterns match E-MORB to N-MORB. Similar geochemical features have been described from the Bransfield Strait, an active spreading Quaternary marginal basin (Keller and Fisk, 1992). Similarity of the Elim Formation samples to these volcanics is evident in the Y-Cr diagram (Fig. 5c), in which they straddle the MORB field, and in respect to shape and absolute abundances in spidergrams. Less altered samples from the Elim Formation show typical features of back arc basalts, such as high Al_2O_3 (>14 wt. %) and low TiO_2 (<1.3 wt. %).

Naub Diorite - Weener Igneous Complex (WIC) - Gaub Valley Formation (GVF)

Only one sample has been taken from the Naub Diorite. However, petrographic studies suggest a similar diversity of igneous rocks as in the WIC. To allow comparison with the latter, samples of the WIC and of the coeval GVF have been included in the present study (Figs. 2 and 4). High affinity to the WIC and the GVF is clearly documented within both scatter and spidergrams and points to an origin as calc-alkaline, subduction-related magma. The pronounced negative Nb, Ta and Ti spikes, as well as strong enrichment of hydrophile elements (Sr to Th) are clear evidence for such origin. The REE pattern coincides with those of the WIC and show flat HREE parallel to CHUR, while LREE increase steeply. A small negative Eu-anomaly (Eu/Eu* = 0.78) excludes any significant contribution of crustal material.

Alberta Complex

Samples were taken from the Marginal Zone (2), the Cone sheet (2), the Basal Zone (6), the Central Zone (7), the Upper Zone (7) and the pyroxenitic rocks (3).

REE patterns from samples within the complex are a combination of the three end members shown in Figure 6. They document that most of the rocks are cumulates with varying proportions of clinopyroxene and plagioclase. Hence, these minerals dominantly control REE distribution of rocks from the magma chamber. The fact that there is no correlation between the absolute concentration of REE and the respective REE pattern is seen as evidence for mixing of trapped and modified melt with cumulate crystals. However, these local processes do not affect the regional character of the Rehoboth Sequence. Therefore, geochemical data from the interior of the complex will be presented and discussed in a separate paper. The generalised N-MORB spidergram of all cumulates is shown in Figure 6. Despite considerable variation, several common characteristics are evident: (1) Elements, except LILE, are moderately to extremely depleted relatively to N-MORB; (2) Most samples show significant negative spikes for HFSE (Th, U, Zr, Nb, Ta, P), while Ti is in line with neighbouring elements; (3) Hump-shaped LILE (Sr, K, Rb, Ba, and Cs) are enriched relatively to the other TE. In contrast to the cumulates from the interior of the complex, rocks from the Marginal Zone are believed, due to more rapid cooling, to approximate parental magma composition. In most Harker diagrams, two of the samples plot in the same domain as analyses from the Elim Formation (Fig. 2). However, increased CaO values are indicative of plagioclase cumulate in sample MZ02. TE and REE patterns (Fig. 4) as well as their ratios of incompatible elements in the Marginal Zone resemble closely those of the Elim Formation.

Discussion and Conclusion

Two problems will be addressed: (1) The possible petrogenetic relationship between the Elim Formation and the Alberta Complex, which is suggested by $^{143}Nd/^{144}Nd$-epsilon values of 0.2 to 4.5 for both units at ~1800 Ma indicating an origin from variably depleted mantle (Ziegler and Stoessel, 1993, Becker *et al.*, subm.), and (2) constraints of the magma chemistry for the plate tectonic setting and evolution of the Rehoboth Sequence.

Petrogenetic relationship between the Elim Formation and Alberta Complex

In order to test whether a petrogenetic relationship exists between the Alberta Complex and the Elim Formation, following assumptions are made: (1) The Alberta Complex and the Elim Formation have a common source; (2) Rocks of the Marginal Zone probably approximate best the parental magma of the Alberta Complex. Cumulate processes are of less importance in that zone than in the interior of the magma chamber; (3) The least evolved sample of the Elim Formation (EFAR04) approximates closely parental magma of the volcanic rocks. Unfortunately, the REE pattern of this sample is rather unstable which probably is due to analytical errors. Therefore, REE concentrations from EFKO05 have been taken for the model composition; (4) Phenocryst assemblage and interstitial liquid have been replaced by metamorphic minerals, and K*d* data from literature (Table 4) had to be used; (5) Parental magma and target composition lie close together on the theoretical crystallisation path. Therefore a constant bulk K*d* can be used for modelling.

It is uncertain whether the Marginal Zone represents a rapidly cooled melt or rather a cumulate rock mixed

Table 4: Partition coefficients K*d* and initial composition SC used for modelling of magma. Compilation of partition coefficients from Rollinson (1993). Initial values are composed of samples from the Areb (EFAR04, Th to Co) and Kobos areas, (EFKO05, REE)

Element	$C^o_1(i)$	Kd [ol]	Kd [cpx]	Kd [opx]	Kd [plag]
La	6.89	0.0067	0.056	0.015	0.19
Ce	16.3	0.0069	0.092	0.02	0.111
Pr	2.29	0.0068	0.161	0.025	0.1005
Nd	10.7	0.0066	0.23	0.03	0.09
Sm	2.87	0.0066	0.445	0.05	0.072
Eu	0.97	0.0068	0.474	0.05	0.443
Gd	3.40	0.0077	0.556	0.09	0.071
Tb	0.56	0.0087	0.57	0.12	0.067
Dy	3.52	0.0096	0.582	0.15	0.063
Ho	0.74	0.0103	0.583	0.19	0.06
Er	2.13	0.011	0.583	0.23	0.057
Tm	0.31	0.0125	0.563	0.285	0.0565
Yb	1.97	0.014	0.542	0.34	0.056
Lu	0.32	0.016	0.506	0.42	0.053
Th	0.47		0.03	0.14	0.01
U	0.15	0.002	0.04	0.01	0.01
Ta	0.39		0.013	0.11	0.03
Nb	5.91	0.01	0.005	0.15	0.01
Zr	67.2	0.012	0.1	0.18	0.048
Hf	1.04	0.013	0.263	0.11	0.051
Ti	8274	0.02	0.4	0.1	0.04
Y	22.56	0.01	0.9	0.18	0.03
V	264	0.06	1.35	0.6	0.022
Sc	33.0	0.17	2.5	1.2	0.01
Co	47.4	6.6	1	3	0.07

with some interstitial melt. Therefore, we have applied two equations from the literature. One describes the evolution of a melt during *in situ* crystallisation (Langmuir, 1989), the other considers the evolution of a solid phase by modified Rayleigh fractionation (Henderson, 1982). We also applied a mere graphical method in order to achieve a good fit of the REE to the target composition (MZ01), to minimise the Eu/Eu* and to keep the composition as close as possible to the CIPW-norm of MZ01 before minimising the trace elements. The original function for *in situ* crystallisation (Langmuir, 1989) has been simplified because two parameters (fA and F) are interdependent. The resulting equations for element (i) are as follows:

(1) K*d*(i)=vol(opx)*K*d*(opx)(i)+vol(cpx)*K*d*(cpx)(i) +vol(ol)*K*d*(ol)(i) + vol(plag)*K*d*(plag)(i)
(2) vol(opx)+vol(cpx)+vol(ol)+vol(plag) = 1
(3) Cl(i) = Col(i)*h^(E(i)-1) with E(i) = 1/(K*d*(i)*(1-f)+f) and h = F^(fA/(fA-1) (Langmuir, 1989)
(4) Cs(i) = Col(i)*[E*(K*d*(i)-1)+1]*F^[E*(K*d*(i)-1)] (Henderson, 1982)

Modelling of major elements has been avoided because of uncertainties in mineral composition. The statistically best fit of the free parameters was calculated using the software program 'Minuit' (1994). The program varies the parameters of a function in order to optimize them, beginning with given initial values, and compares theoretical results with the real data set. Normally, the parameters eventually converge on a global minimum, which corresponds with the nearest distance between real world and theory. In addition, chi^2, which is a measure for the likelihood of the hypothesis, is calculated from the error matrix of the data set. It is, however, largely dependent not only on the function itself but also on the data errors. In this study, relative errors of 10% were assigned to REE, 30% to TE and 40% to Hf and Zr. These are probably minimum values, which integrate analytical uncertainties, uncertainties in K*d*, as well as data scatter resulting from geological processes (e.g. metamorphism, weathering). In this case values of chi^2 above 2.0 would suggest that the hypothesis is unlikely, with a 2 sigma confidence level, and should be rejected.

The parameters of the best fits are given in Table 5, with the resulting spidergrams shown in Figure 7 (model composition is normalised by the real data of sample MZ01 from the Marginal Zone). Using the model of *in situ* crystallisation we obtained a relatively good fit (chi^2 = 1.2) with a low degree of fractionation from the parental magma (h = 0.968) and a minor solidification zone (f = 0.012). Therefore, it seems likely that the Marginal Zone represents a liquid derived from a parental magma of subalkaline tholeiitic composition. In contrast, the higher chi^2 value (1.86), as well as the unrealistically high degree of fractionation (f=0.237) in the Marginal Zone argues against Henderson's model of a cumulate with some trapped supernatant melt. Finally, the 'common sense' approach by graphical means yielded reasonable parameters for both proportions of the minerals involved in crystallization, as well as degree of fractionation (0.62) and mixing of cumulate (0.62) with liquid (0.38). However, the high chi^2 of 4.0 again shows rather limited likelihood that this hypothesis applies.

Despite many uncertainties modelling shows that there is a high affinity between the Marginal Zone of the Alberta Complex and the Elim Formation. Alternatively, the good fit of the model and the real data probably can be obtained by enhanced assimilation of country rock within that zone, a model which still needs to

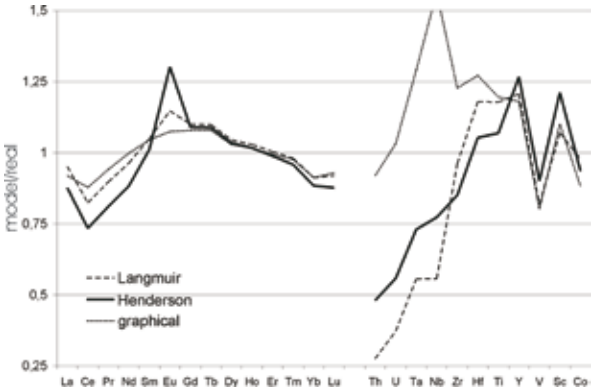

Figure 7: Results of modelling, REE and TE, applying different functions.

Table 5: Presentation of 'best fit' parameters and chi^2 using different models

Author	Method	Equations used for optimisation	vol(ol)	vol(opx)	vol(cpx)	vol(plag)	f	h	chi^2/n
Langmuir (1989)	Minuit	(1), (2), (3)	0.51	0.00	0.12	0.37	0.012	0.968	1.2
							F	E	
Henderson (1982)	Minuit	(1), (2), (4)	0.01	0.00	0.27	0.7269	0.237	0.925	1.86
	Graphical	(1), (2), (4)	0.00	0.10	0.30	0.60	0.620	0.620	4.0
CIPW-norm			0.04	0.18	0.12	0.62			

be tested.

Constraints of magma geochemistry for plate tectonic setting and evolution of the Rehoboth Sequence

Petrographic studies of Palaeoproterozoic units from the Rehoboth Basement Inlier together with geochemical data of igneous rocks provide important constraints for the evolution of this crustal segment. Field observations, geochemistry, geochronology and isotope systematics ($^{87}Sr/^{86}Sr$ initials) suggest coeval evolution of the Gaub Valley Formation and the WIC within a subduction-related environment (Becker, 1995; Nagel *et al.*, 1996; Becker *et al.*, 1996; Becker *et al.*, subm). Recent fieldwork shows that metatuffites of the Gaub Valley Formation grade into clastic and epiclastic sediments of the Elim Formation which are intruded by calc-alkaline magmas. Higher up in the stratigraphy, a succession of shallow marine chert, magnetite quartzite and metacarbonate is interlayered with hyaloclastic mafic volcanics and quartz-mica schist. Geochemical analyses of the volcanic rocks reveal a tholeiitic, subalkaline character with affinity to E-MORB, which is typical for back arc related basalts. Hence, change from subduction-related volcanism in the Gaub Valley Formation to back-arc related volcanism of the Elim Formation must have occurred fairly rapidly during opening of the back arc. Geochemical characteristics of the Alberta Complex show high affinity to the Elim Formation and indicates emplacement of this intrusion during the same magmatic event. In summary, Figure 8 shows the hypothetical evolution of the Rehoboth Sequence within an arc - back arc system and sources of different magma types. Early stage igneous rocks such as the WIC, Gaub Valley volcanics and Naub Diorite show clearly subduction zone influence both in spider and ratio-ratio diagrams. Decreasing influence of arc magmatism and derivation from enriched mantle is indicated for the Elim Formation by lower Nb/Yb and Th/Yb ratios, together with TE patterns typical for back-arc regions. Intrusion of the Alberta Complex may be assumed during this stage from a slightly more residual mantle.

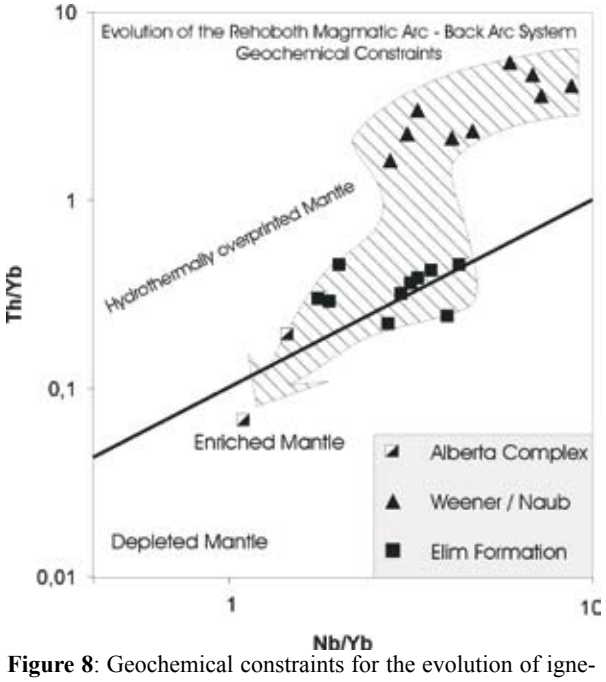

Figure 8: Geochemical constraints for the evolution of igneous rocks of the Rehoboth Sequence

Acknowledgements

TB would like to thank T. Oberthuer of the Federal Institute for Geoscience and Natural Resources (BGR) Hannover who made possible the analysis of samples from the Alberta Complex and the Kobos area. A. Boehm carried out geochemical analyses of amphibolites from the farm Areb and together with K. Weber is thanked for permission to use these data. Research was carried out in collaboration with the Geological Survey of Namibia. S.A. De Waal, D. Reid and U. Schreiber provided many helpful comments and suggestions on a first draft of the manuscript.

References

Becker, T. 1995. *Die Geologie, Geochemie und Geochronologie des Weener Igneous Komplex und der Gaub Valley Formation in der Südlichen Randzone des Damara Orogens, Namibia und ihre Bedeutung für die Entwicklung der frühproterozoischen Rehoboth Sequenz*. Cuvillier, Göttingen, 250 pp.

Becker, T. Hansen, B.T., Weber, K. and Wiegand, B. 1996. U-Pb and Rb-Sr isotopic data of the Mooirivier Complex, the Weener Igneous Suite and the Gaub Valley Formation (Rehoboth Sequence), Nauchas area, and their significance for the Paleoproterozoic evolution of Namibia. *Communs geol. Surv.*

Namibia, **11**, 31-46.

Becker T., Diedrichs, B., Hansen B.T. and Weber, K. 2000. Implications from geochemical systematics of the Weener Igneous Complex for the evolution of the Paleoproterozoic Rehoboth Basement Inlier (Namibia). *Communs geol. Surv. Namibia*, (this volume).

Boehm, A. 1998. *Geochemische Untersuchungen an basischen und felsischen prae-damarischen Gesteinen am Suedrand des Damara Orogens (Farm Areb), Namibia*. Unpubl. Diplom thesis, Univ. Goettingen, 62 pp.

Brewitz, H.W. 1974. Montangeologische Erkundung und Genese der metamorphen, exhalativ-sedimentären Zn-Cu-Lagerstätte Kobos im Altkristallin des Nauchas Hochlandes, SW-Afrika. *Clausthaler Geol. Abh.*, **18**, 128 pp.

Burger, A.J. and Walraven, F. 1978. Summary of age determinations carried out in the period April 1974 to March 1975. *Ann. geol. Surv. S. Afr.*, **11**, 317-322.

Cabanis, B. and Lecolle, M. 1989. Le diagram La/10-Y/15-Nb-8: un outil pour la discrimination des series volcaniques et la mise en evidence des processus de melange et/ou de contimination crustale. *C.r. Acad. Sci. Ser. II*, **309**, 2023-2029.

De Waal, S.A. 1966. *The Alberta Complex, a metamorphosed layered intrusion north of Nauchas, SWA, the surrounding granites and repeated folding in the younger Damara system*. Unpubl. D.Sc. thesis, Univ. Pretoria, 203 pp.

Fryer. P., Taylor, B., Langmuir, C.H. and Hochstaedter, A.G. 1990. Petrology and geochemistry of lavas from the Sumisu and Torishama back arc rifts. *Earth Planet. Sci. Lett.*, **100**, 161-178.

Gribble R.F., Stern, J.S., Newman, S., Bloomer, S.H. and O'Hearn T. 1998. Chemical and isotopic composition of lavas from the northern Mariana trough: implications for magmagenesis in back-arc basins. *J. Petrol*., **39**, 125-154.

Heinrichs, H. and Herrmann, A.G. 1990. *Praktikum der analytischen Geochemie*. Springer Verlag, Berlin, 669 pp.

Hofmann, A.W. 1988. Chemical differentiation of the Earth: the relationship between mantle, continental crust, and oceanic crust. *Earth Planet. Sci. Lett*., **90**, 297-314

Hilken, U.1998. *Die Altersstellung von metamorphen prae-Damara Plutoniten und Vulkaniten am Suedrand des Damara Orogens, Farm Areb 176, Namibia, abgeleitet aus U/Pb-Isotopenuntersuchungen*. Unpubl. Diplom thesis, Univ. Goettingen, 55 pp.

Keller R.A.and Fisk M.R. 1992. Quarternary marginal basin volcanism in the Bransfield Strait as a modern analogue of the southern Chilean ophiolites. *In*: Parson, L.M., Murton, B.J. and Browning, P. (eds) *Ophiolites and their modern oceanic analogues*. Spec. Publ. geol. Soc., **60**, 155-169.

Maillet, P. and 8 co-authors. 1995. Tectonics, magmatism, and evolution of the New Hebrides back arc troughs (Southwest Pacific). *In*: Taylor (ed.) *Back-arc Basins. Tectonics and Magmatism*. Plenum Press, New York, 176-235.

Master, S. 1993. Early Proterozoic assembly of "Ubendia" (Equatorial and Southern Africa and adjacent parts of South America): tectonic and metallogenic implications. Symposium Early Proterozoic, Geochemical and Structural constraints-metallogeny. *CIFEG Occ. Publ., Dakar,* **23**, 103-107.

MINUIT-Function Minimization and Error Analysis, Version 94.1. 1994. *Program Library entry D506, CERN, Geneva*.

Nagel, R., Warkus, F., Becker, T. und Hansen, B.T. 1996. U/Pb-Zirkondatierungen der Gaub Valley Formation am Südrand des Damara Orogens/Namibia und ihre Bedeutung für die Entwicklung des Rehoboth Basement Inlier. *Zt. Geol. Wiss*., **24**, 611-618.

Pearce J.A. and Cann J.R. 1973. Tectonic setting of basic volcanic rocks determined using trace element analyses. *Earth Planet. Sci. Lett*., **19**, 290-300.

Pearce, J.A. 1982. Trace element characteristics of lavas from destructive plate boundaries. *In*: Thorpe (ed.), *Andesites*. Wiley, Chichester, 525-548.

Pfurr, N., Ahrendt, H., Hansen, B.T. and Weber, K. 1991. U-Pb and Rb-Sr isotopic study of granitic gneisses and associated metavolcanic rocks from the Rostock massifs, southern margin of the Damara Orogen: implications for lithostratigraphy of this crustal segment. *Communs geol. Surv. Namibia*, **7**, 35-48.

Reid, D.L., Malling, S. and Allsopp, H.L. 1988. Rb-Sr ages of granitoids in the Rehoboth-Nauchas area SWA/Namibia. *Communs geol. Surv. Namibia*, **4**, 19-28.

Rollinson, H. 1993. *Using geochemical data: evaluation, presentation, interpretation*. Longman, Singapore, 352 pp.

Schalk, K.E.L. 1988. Pre-Damaran basement rocks in the Rehoboth and Southern Windhoek districts (areas 2217D, 2316, 2317A-C) - a regional description. *Unpubl. Rep. geol. Surv. S.W.Afr./Namibia*, Windhoek.

Shervais J.W. 1982. Ti-V plots and the petrogenesis of modern and ophiolitic lavas. *Earth Planet. Sci. Lett*., **59**, 101-118.

Winchester J.A. and Floyd, P.A. 1977. Geochemical discrimination of different magma series and their differentiation products using immobile elements. *Chem. Geol*., **20**, 325-343.

Ziegler, U.R.F and Stoessel, G.F.U. 1993. Age determinations in the Rehoboth Basement Inlier, Namibia. *Mem. geol. Surv. Namibia*, **14**, 106 pp.